Free-form optics for Fresnel-lens-based photovoltaic concentrators

Juan C. Miñano,[1,2,*] Pablo Benítez,[1,2] Pablo Zamora,[1] Marina Buljan,[1] Rubén Mohedano,[2] and Asunción Santamaría[1]

[1]*Universidad Politécnica de Madrid, Cedint, Campus de Montegancedo, Madrid 28223, Spain*
[2]*LPI, 2400 Lincoln Ave., Altadena, CA 91001, USA*
[*]*jc.minano@upm.es*

Abstract: The Concentrated Photovoltaics (CPV) promise relies upon the use of high-efficiency triple-junction solar cells (with proven efficiencies of over 44%) and upon high-performance optics that allow for high concentration concurrent with relaxed manufacturing tolerances (all key elements for low-cost mass production). Additionally, uniform illumination is highly desirable for efficiency and reliability reasons. All of these features have to be achieved with inexpensive optics containing only a few (in general no more than 2) optical elements. In this paper we show that the degrees of freedom using free-forms allow the introduction of multiple functionalities required for CPV with just 2 optical elements, one of which is a Fresnel lens.

OCIS codes: (220.1770) Concentrators; (350.6050) Solar energy; (040.5350) Photovoltaic; (220.4298) Nonimaging optics; (220.4610) Optical fabrication; (220.2740) Geometric optical design.

References and links

1. R. Winston, J. C. Miñano, and P. Benítez, *Nonimaging optics*, (Elsevier Academic Press, Burlington, MA, 2005)
2. P. Benitez and J. C. Miñano, "Concentrator Optics for the next generation photovoltaics". in *Next Generation Photovoltaics: High Efficiency through Full Spectrum Utilization*, A. Marti, A. Luque, ed. (Taylor & Francis, CRC Press, London, 2004)
3. A. Luque, *Solar Cells and Optics for Photovoltaic Concentration*, (Adam Hilger, Bristol, UK, 1989)
4. P. Benítez, J. C. Miñano, P. Zamora, R. Mohedano, A. Cvetkovic, M. Buljan, J. Chaves, and M. Hernández, "High performance Fresnel-based photovoltaic concentrator," Opt. Express **18**(S1), A25–A40 (2010).
5. N. Shatz, J. Bortz, and R. Winston, "Thermodynamic efficiency of solar concentrators," Opt. Express **18**(S1), A5–A16 (2010), doi:10.1364/OE.18.0000A5.
6. J. C. Miñano, M. Hernández, P. Benítez, J. Blen, O. Dross, R. Mohedano, and A. Santamaría, "Free-form integrator array optics," Proc. SPIE **5942**, 59420C, 59420C-12 (2005), doi:10.1117/12.620240.
7. J. C. Miñano and J. C. González, "New method of design of nonimaging concentrators," Appl. Opt. **31**(16), 3051–3060 (1992).
8. P. Benítez, J. C. Miñano, J. Blen, R. Mohedano, J. Chaves, O. Dross, M. Hernández, J. L. Alvarez, and W. Falicof, "Simultaneous multiple surface optical design method in three dimensions," Opt. Eng. **43**(7), 1489–1502 (2004).
9. http://www.lpi-llc.com/pdf/Ventana2012.pdf
10. http://corporate.evonik.com/en/media/press_releases/pages/news-details.aspx?newsid=26669
11. P. Zamora, P. Benítez, R. Mohedano, A. Cvetković, J. Vilaplana, Y. Li, M. Hernández, J. Chaves, and J. C. Miñano, "Experimental characterization of Fresnel-Köhler concentrators," J. Photon. Energy. **2**(1), 021806 (2012), doi:10.1117/1.JPE.2.021806.
12. M. Buljan, P. Benítez, R. Mohedano, and J. C. Miñano, "Improving performances of Fresnel CPV system: Fresnel-RXI Köhler concentrator", *Proceedings of 25th EU PVSEC*, (2010) pp. 930–936. http://dx.doi.org/10.4229/25thEUPVSEC2010-1DV.5.26.
13. P. Zamora, A. Cvetkovic, M. Buljan, M. Hernández, P. Benítez, J. C. Miñano, O. Dross, R. Alvarez, and A. Santamaría, "Advanced PV Concentrators", in *Proceedings of Photovoltaic Specialists Conference (PVSC), 2009 34th IEEE* (Institute of Electrical and Electronics Engineers, New York, 2009) pp. 929–932, http://dx.doi.org/10.1109/PVSC.2009.5411135
14. A. Cvetkovic, R. Mohedano, P. Zamora, P. Benitez, J. C. Miñano, J. Chaves, M. Hernandez, and J. Vilaplana, "Characterization of Fresnel-Köhler concentrator", *Proceedings of 25th EU PVSEC*, (2010), pp 176–181, (2010). http://dx.doi.org/10.4229/25thEUPVSEC2010-1BO.7.6
15. M. Hernandez, A. Cvetkovic, P. Benitez, J. C. Miñano, W. Falicoff, Y. Sun, J. Chaves, and R. Mohedano, "CPV and illumination systems based on XR-Köhler devices", in Nonimaging Optics: Efficient Design for Illumination

#183585 - $15.00 USD Received 16 Jan 2013; revised 11 Mar 2013; accepted 12 Mar 2013; published 22 Apr 2013

and Solar Concentration VII, ed. Roland Winston, Jeffrey M. Gordon, Proc. SPIE **7785**, 77850A (2010). http://dx.doi.org/10.1117/12.861968.
16. S. Kurtz and M. J. O'Neill, "Estimating and controlling chromatic aberration losses for two-junction, two-terminal devices in refractive concentrator systems", *Proceedings of Photovoltaic Specialists Conference (PVSC), 1996 25th IEEE* (Institute of Electrical and Electronics Engineers, New York, 1996), pp. 361–364, (1996). http://dx.doi.org/10.1109/PVSC.1996.564020.
17. P. Zamora, P. Benitez, Y. Li, J. C. Minano, J. Mendes-Lopes, and K. Araki, "The dome-shaped Fresnel-Köhler concentrator" in AIP Conf. Proc. 1477, **69** (2012), http://dx.doi.org/10.1063/1.4753836
18. P. Zamora, P. Benítez, L. Yang, J. C. Miñano, J. Mendes-Lopes, and K. Araki, "Photovoltaic performance of the dome-shaped Fresnel-Köhler concentrator," Proc. SPIE **8468**(84680D), 84680D (2012), doi:10.1117/12.929698.
19. J. C. Miñano, J. C. Gonźlez, and P. Benítez, "A high-gain, compact, nonimaging concentrator: RXI," Appl. Opt. **34**(34), 7850–7856 (1995), doi:10.1364/AO.34.007850.
20. P. Benítez, J. C. Miñano, J. Blen, R. Mohedano, J. Chaves, O. Dross, M. Hernández, J. L. Alvarez, and W. Falicoff, "Simultaneous multiple surface optical design method in three dimensions," Opt. Eng. **43**(7), 1489–1502 (2004), doi:10.1117/1.1752918.
21. http://www.soitec.com/en/solar-energy/
22. L. W. James and W. James, "Use of imaging refractive secondaries in photovoltaic concentrators", Contractor Report SAND89–7029, Sandia Labs, Albuquerque, New Mexico, (1989)
23. *http://www.amonix.com*
24. http://www.solfocus.com/

1. Introduction

Minimizing energy cost (€/kWh) is a necessary task for the success of Concentrated Photovoltaics (CPV). Key to minimizing this cost is an efficient and low-cost optical concentrator, with a high concentration (>500) that allows for rapid amortization of the cost of high-efficiency triple-junction solar cells. A low-cost concentrator is best met with the fewest elements and the most relaxed manufacturing and assembling tolerances. These tolerances can be expressed in terms of the concentrator's acceptance angle α [1], specifically higher the acceptance angle, more the relaxed tolerances of the concentrator. A useful merit function for a CPV optic is the concentration-acceptance product [2], defined as:

$$CAP = \sqrt{C_g}\sin(\alpha) \tag{1}$$

where C_g is the geometric concentration and α the acceptance angle, defined as the incidence angle at which the concentrator collects 90% (sometimes 95%) of the on-axis power [3]. A more practical definition says that it is the angle at which the generated photocurrent is at 90% of the maximum (typically achieved at normal incidence). In terms of generated electric power, a more useful definition would be the angle at which the maximum electric power generated by the cell P_{MPP} (moving along the *I-V* curve) is at 90% of the maximum electric power generated by the cell at the best incidence angle. This is usually referred to as the effective acceptance angle. This definition takes into account all optical and electrical effects.

In this paper we will use the first definition of α which is not dependent on the cell behavior. It is remarkable that for a given concentrator architecture, this *CAP* is practically constant. This definition of *CAP* is close to the concept of Numerical Aperture (*NA*) in Imaging Optics, but is not exactly the same. *NA* is either the sine of the acceptance cone of an objective, or refers to the maximum angle of acceptance (or illumination) of a ray bundle transmitted by a fiber. *NA* and *CAP* definitions coincide when every point of the cell is illuminated by light cones with the same angle, which is an unlikely ideal case. The *CAP* is not the sine of the maximum angle of the cone of light transmitted to the cell, but the maximum angle of such an ideal illumination enclosing the same etendue. The *CAP* (as well as the *NA*) is upper bounded by the refractive index of the medium surrounding the cell, which is typically a silicone of n≈1.42. For details about the thermodynamic upper limit of the *CAP* see for instance [2, 4, 5].

For a given C_g, the acceptance angle α also measures the total tolerance available to apportion among the different imperfections of the system, namely: (1) shape errors and roughness of the optical surfaces, (2) concentrator module assembly, (3) array installation, (4) tracker structure finite stiffness, (5) sun-tracking accuracy, (6) solar angular diameter, (7) lens warp, and (8) soiling. Each of these imperfections can be expressed as a fraction of the

#183585 - $15.00 USD Received 16 Jan 2013; revised 11 Mar 2013; accepted 12 Mar 2013; published 22 Apr 2013

tolerance angle, so that, all together, they comprise a "tolerance budget". Alternatively, for a given acceptance angle, a higher *CAP* allows a higher concentration, consequently reducing required cell size (and cost). The actual impact of *CAP* on receiver costs has been analyzed in ref [4] by comparing several Fresnel-based systems.

In this paper, we will present the progress in the development of the most advanced CPV optical designs that use a Fresnel lens as the Primary Optical Element (POE). These are based on free-form array optics using Köhler integration. The fundamentals of the general design procedure were described in [6]. The main idea is to use arrays of different Köhler integrators designed on an SMS optic [7, 8]. Each one of these Köhler integrators comprises two optical surfaces which may be free-form (i.e. without rotational symmetry). The degrees of freedom of using free-form surfaces allow for the introduction of multiple functionalities in the optical surfaces. Specifically, these provide a high *CAP* with excellent light homogenization for any sun position within the acceptance angle. The two surfaces forming any Köhler pair are usually placed into two different elements: one in the POE; and another one in the Secondary Optical Element (SOE). Even though the optical designs are sometimes complex, the elements can be manufactured with the same techniques as classical design optics (typically plastic injection molding, embossing, casting, and glass molding) and therefore their production cost is the same as non-free-form elements.

SOEs designs like the inverted truncated pyramid (also called RTP), the kaleidoscopic prism and those of the CPC family require the reflective surface to extend till the cell active surface, i.e., there is a region of the cell very close to the reflector. This fact becomes a problem in those dielectric filled SOEs whose reflectors are based in total internal reflection (TIR). This is because, the agent which typically couples the SOE and the cell may be either in excess or less, leading to optical losses, either because the TIR in the SOE reflector fails (excess) or because a TIR reflection appears at the cell-SOE interface (lack). The coupling agent is usually silicone. The concentrators presented here do not have this problem: no optical surface is in contact with the edge of the cell. Since glue (and light) leakage is not a concern anymore, the SOE-to-cell optical coupling process becomes much easier and enables low-cost high-yield encapsulation in mass production. It also allows for high reliability encapsulation schemes where the path from any point of the cell to the air can be long and filled with non permeable material. Also, the optical coupling media on top of the cell surface can be liquid because it does not have any structural function. In the latter case, there are non-optically-active parts of the SOE that are used to contain the elements and for mechanical attachment.

Two different design families for the concentrators are presented. The first one (FK, in Section 2) uses a single refracting surface as a secondary optic while the second (F-RXI in Section 3) uses an RXI for the same function. The FK is already on the market [9, 10] and has experimentally proven module electrical (DC) efficiencies of 32.7% (at T_{cell} = 25°C) with a concentration of 710x and a tolerance angle $\alpha = \pm 1.27°$ (*CAP* = 0.59) and without any anti-reflective (AR) coating on the optics [11]. Ray-tracing simulations showing optical efficiency, angular transmission (and *CAP*), and irradiance distribution are included in this paper. A comparative study of the designs discussed in this paper and those of classical designs is also presented in Section 4. More details of these devices can be found in [4, 12–14]. CPV concentrators using Köhler array schemes but with a mirror as the POE can be found in [15].

#183585 - $15.00 USD Received 16 Jan 2013; revised 11 Mar 2013; accepted 12 Mar 2013; published 22 Apr 2013

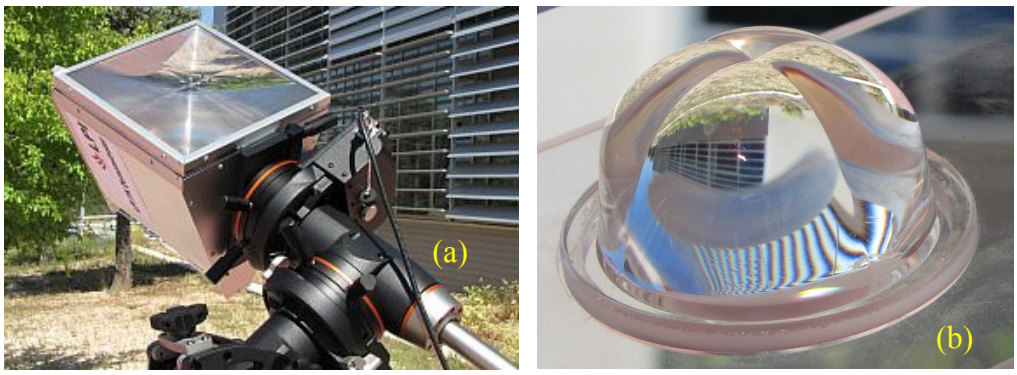

Fig. 1. A 4-sector FK concentrator during measurements (a) and its glass molded SOE (b) showing the second part of the four sectors of the Köhler array.

2. The FK concentrator

The FK (Fresnel Köhler concentrator) consists of a Fresnel lens comprising of four identical folds or quadrants, along with a free-form secondary lens, also divided into four equal sectors (see Fig. 1). Each POE + SOE quadrant pair works together as a Köhler integrator couple. Using the standard nomenclature for these nonimaging devices [15], the name should be RR, which indicates that the two designed surfaces (the Fresnel facets and the SOE upper surface) are refractive. Using the Köhler integration principle, each quadrant of the POE images the sun on its corresponding counterpart sector in the SOE, while the SOE sector images the POE ray bundle onto the cell, producing a uniform square spot onto it.

The FK attains unique performance features, such as reduced optical depth (for the same performance), a very good *CAP* (*CAP* = 0.59) and almost perfect irradiance uniformity over the solar cell. The *CAP* is not at the thermodynamic upper limit (≈1.42), but still much beyond conventional Fresnel concentrators as shown in Section 4.

The irradiance uniformity occurs not only when the whole spectrum is considered but also when it is restricted to the top or middle subcell ranges as can be seen in Fig. 2 below. This last result is very important in order to avoid conversion efficiency losses due to chromatic mismatch [16]. For further details see [4] and [9].

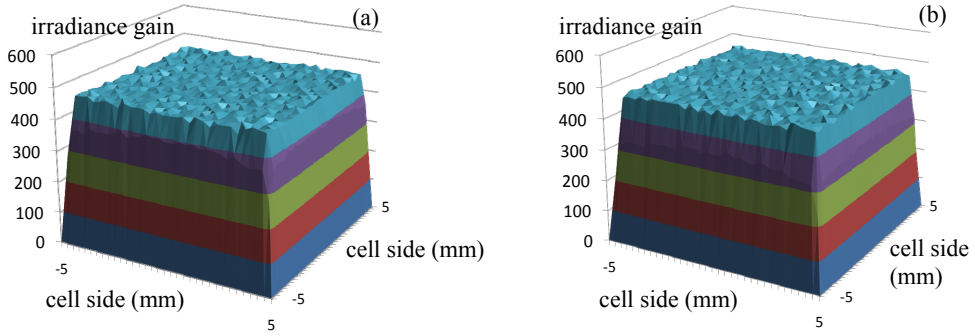

Fig. 2. Simulated irradiance distribution on the cell for the FK concentrator with parameters Cg = 625x, f/0.85, when the sun is on axis and the solar spectrum is restricted to: (a) the top-subcell range (360-690 nm), and (b) the middle-subcell range (690-900 nm). The vertical axis denotes the irradiance gain of the respective wavelength ranges relative to the 1-sun case.

#183585 - $15.00 USD Received 16 Jan 2013; revised 11 Mar 2013; accepted 12 Mar 2013; published 22 Apr 2013

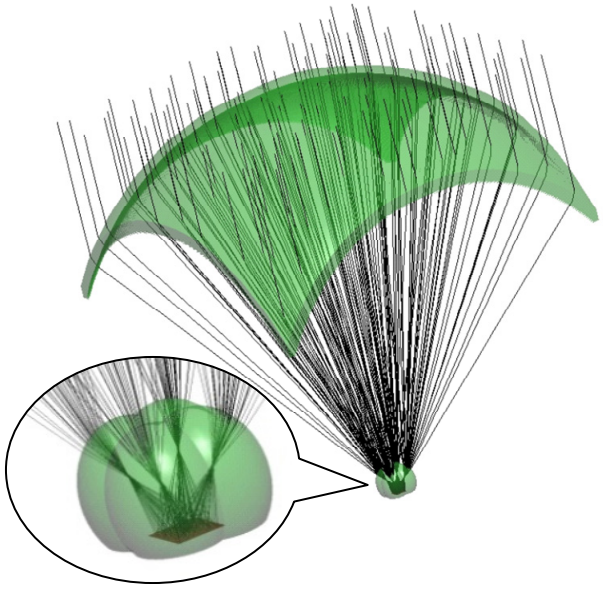

Fig. 3. Rendered view of a dome-shaped FK concentrator (DFK). At bottom left, a detailed view of the SOE, where the 4 sectors can be distinguished, each one receiving light from one of the POE sectors.

Recently, an FK concentrator with a dome-shaped Fresnel lens has been designed and manufactured [17, 18] (see Fig. 3). The dome-shaped Fresnel lens also forms a Köhler array integrator with its SOE. This device is called DFK. Its *CAP* is quite high (0.72), leading to a C_g = 1,230x and an acceptance angle of ± 1.18°. The expected optical efficiency of this DFK is 85.6% (without AR coating on the optics). The irradiance distribution on the cell is not as uniform as the flat Fresnel case FK (see Fig. 4). The spot on the cell is also square.

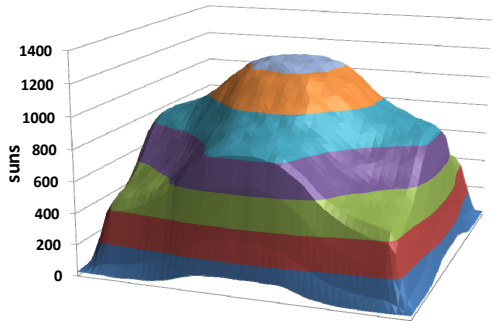

Fig. 4. DFK concentrator: Irradiance distribution on the cell, when illuminating the DFK at normal incidence with 1 sun irradiance.

2.1 Outdoor measurements of an FK concentrator

The FK prototype shown in Fig. 1 was measured outdoors. The prototype consists of a PMMA Fresnel lens, with an active area of 144 cm^2, a B270 glass-molded SOE (without AR coating) coupled to the cell with a transparent silicone rubber layer (Sylgard 182 by Dow Corning, with refractive index = 1.41) and a high efficiency (≈38%) 1 cm^2 commercial triple-junction Spectrolab cell mounted on an aluminum heatsink.

Measurements on this prototype showed an efficiency of 32.7% and a fill-factor of 84.6% for a cell temperature of T_{cell} = 25°C. These measurements were performed under a DNI of 835W/m^2.

#183585 - $15.00 USD Received 16 Jan 2013; revised 11 Mar 2013; accepted 12 Mar 2013; published 22 Apr 2013

Acceptance angle measurement results are shown in Fig. 5(a). Measurements for this calculation were done under a DNI of 975W/m^2. With a sun incidence of ± 1.24° the FK efficiency drops off to the 90% of its nominal value, which is just 0.01° less than the simulated result (see comparative curves in Fig. 5(a)). It can be observed that the simulated and measured curves, besides having a similar acceptance angle, have the same pill-box shape. On Fig. 5(b), a picture of the SOE back surface is shown in which the solar cell has been replaced by a transmissive diffuser. The figure shows the characteristic square spot of an FK concentrator. More details of these experimental results can be found in [11].

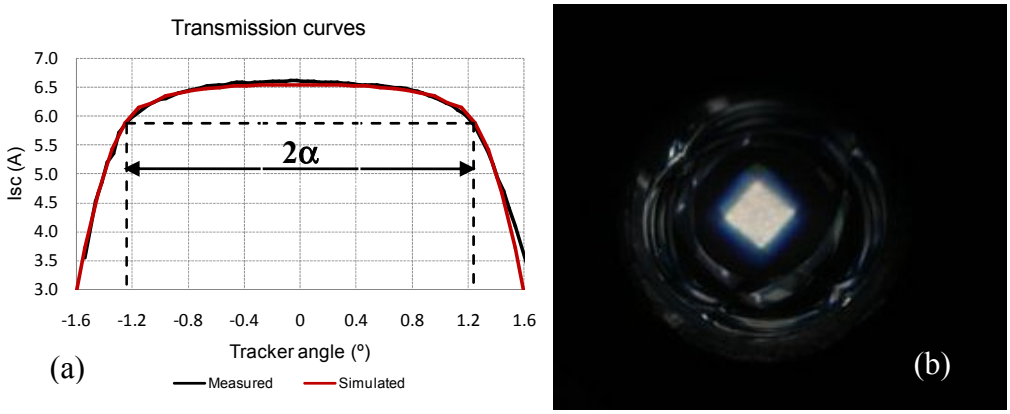

Fig. 5. Simulated and measured transmission curves (a) with α_{sim} = ± 1.25° and $\alpha_{measured}$ = ± 1.24°. Illuminated SOE back surface (b) where the cell has been substituted by a transmissive diffuser.

3. The F-RXI concentrator

In this section we will show a more advanced design, which also uses a flat Fresnel lens as a primary. This device is also 4-fold and uses an RXI as the SOE. The RXI surfaces are calculated using the SMS design method in 3D. In this SOE, the rays undergo refraction (R), reflection (X) and total internal reflection (I). For these reasons, the SMS nomenclature for this device is "RXI" assigning letters to each surface that deflects rays. The RXI is a solid dielectric piece that has a small metallized surface on the front (optional) and a larger metallized surface on the back which act as mirrors. The RXI is a well-known device in the field of Nonimaging Optics. It was first designed with rotational symmetry [1, 19] and later with free-form surfaces for automotive applications [20].

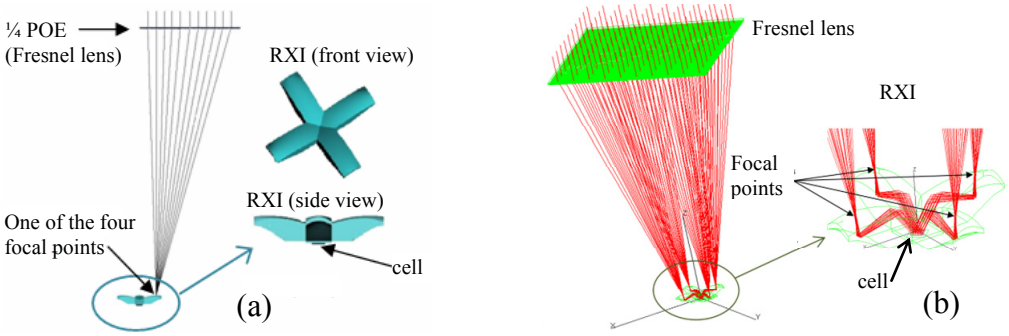

Fig. 6. (a) Scheme of the normal-incidence rays passing through one quarter of the POE (Fresnel lens) and focusing on the corresponding surface of the SOE (RXI). Light is focused by each Fresnel lens quarter on four different foci (b), corresponding to the four SOE parts.

Figure 6(a) shows the normal-incidence rays passing through one quarter of a Fresnel POE and focusing on the corresponding upper surface of the SOE, which, as said before, is an

#183585 - $15.00 USD Received 16 Jan 2013; revised 11 Mar 2013; accepted 12 Mar 2013; published 22 Apr 2013

RXI. The figure also shows two views of the RXI (in blue). Figure 6(b) shows the complete ray-traced trajectories of some rays also hitting the Fresnel lens perpendicularly. This ray bundle is split by the four-quadrant Fresnel lens and focused onto the four SOE parts, to be spread afterwards to produce uniform irradiance on the solar cell. This applies for every ray within a design acceptance angle ± α.

The RXI design uses an iterative process in which the R and I surfaces are treated as two separate surfaces. An initial shape for the surface R is chosen (R_0) and the SMS 3D method is applied to calculate surfaces X and I. Next, the calculated surface I is considered a new R surface (R_1) and the design is done again to recalculate new surfaces X and I. The process is repeated until the sequence of surfaces R_n converges towards the final design surface. This iterative process is peculiar to the RXI when compared to other SMS devices, and arises from the circumstance that two distinct optical surfaces, the chosen surface R and the calculated surface I, must converge to the same physical surface.

The relevance of this novel design comes from the *CAP* it generates. Two variants of the concentrators comprised by an RXI as their secondary optical element will be considered below. The first one has an RXI secondary with the small frontal area metallized. It has a value for *CAP* = 0.85. In the second case, the RXI does not have the frontal metallization, in order to make the device easier to manufacture. This latter one reaches a lower *CAP* value of 0.73, which is just a bit greater than the *CAP* of the dome-shaped Fresnel lens FK shown in section 2, Fig. 3. These two F-RXI designs have the highest reported values for *CAP* among concentrators based on Fresnel lenses.

3.1 Simulation results

The first concentrator we have considered is an F-RXI with an *f*-number 1.4 and a geometrical concentration of C_g = 2,300x. As said before, the secondary optical element (RXI) has a small frontal metallized area. This F-RXI has the following additional parameters: (i) Fresnel lens: area = 852.64 cm^2 made of PMMA (n≈1.49), facet draft angle = 2°; (ii) Dielectric SOE: BK7 glass (n≈1.51872) with mirror reflectivity of 0.97. The optical efficiency derived from ray tracing using this data is 82.5%, which can be increased to 85% with AR coating of the RXI front face.

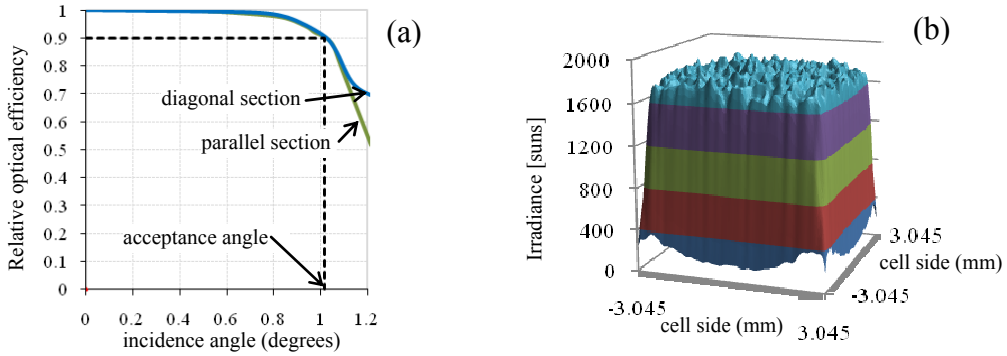

Fig. 7. Simulation showing the relative optical efficiency versus incidence angle on a 2,300x free-form F-RXI Köhler concentrator (a). The resulting acceptance angle is α = ± 1.02°. The irradiance distribution on the cell when the sun's center is at normal incidence (@DNI = 1 sun) is shown in (b).

The relative optical efficiency (i.e., the relative transmission) is shown in Fig. 7(a) with dashed lines highlighting the acceptance angle ± 1.02°. Curves for transmission in a plane parallel to the sides of the square Fresnel primary lens (referred to as "parallel") and in a plane parallel to the diagonal of the square Fresnel primary lens (referred to as "diagonal") are provided. A *CAP* = 0.85 is achieved. This F-RXI concentrator also produces excellent irradiance uniformity on the cell. Figure 7(b) shows the irradiance distribution on the cell when the sun is on-axis with a Direct Normal Irradiance (DNI) of 850 W/m^2.

#183585 - $15.00 USD Received 16 Jan 2013; revised 11 Mar 2013; accepted 12 Mar 2013; published 22 Apr 2013

As mentioned above, the RXI of the second F-RXI concentrator considered here has no frontal metallized area. All other design parameters are the same as the first case. The simulation results show an acceptance angle of ± 0.87°, which implies a *CAP* = 0.73. According to the simulation, the optical efficiency (considering Fresnel losses, absorption losses and RXI back mirror reflectivity) is 83.5%, which can be increased to 86% with AR coating on the RXI front face.

4. Comparison

A comparison of the FK and F-RXI concentrator families described herein with five other, more conventional CPV concentrator families that use a flat Fresnel lens as a primary optical element is presented. All the concentrators chosen for the comparison have the same Fresnel POE entry aperture area (625 cm^2), the same acceptance angle (α = ± 1°), but different concentration ratios (and thus different cell sizes). This makes it easier to compare them, since the cost differences will arise only from the combination of cell and SOE costs. Both the Fresnel lens and the solar cell active area are square. First, we considered a Fresnel lens concentrator with no SOE, which is a type of system being used now by the company Soitec [21]. In the second case, we considered an SOE with a hemispherical glass dome centered on the cell surface and in optical contact with it. This type of dome concentrator has been proposed as a candidate for improving the *CAP* of the preceding case. Thirdly, we selected for this comparison a SILO (SIngLe Optical surface) SOE, designed by James for Sandia Labs in the 90's [22]. This concentrator has a single Köhler channel. The SILO design we have used in this comparison is the one providing maximum *CAP* which is not exactly the same proposed by James. The fourth SOE considered was a hollow reflective truncated pyramid (XTP), which is the type of SOE presently being used by the company Amonix [23]. The fifth approach was a solid dielectric truncated pyramid (RTP), which works by total internal reflection. This type of SOE is used in several commercial products (for instance, by the company Solfocus [24]). In the case of the F-RXI, both designs introduced in section 3 are considered: one with a small metallized frontal area (labeled FRXI), and the other without frontal metallization (labeled FRXI*).

The true-scale relative size comparison among the different SOEs can be seen in the cross sectional drawings of Fig. 8. The *f*-numbers and the geometrical concentrations of the different configurations are shown in the same figure.

concentrator type	*f*-number	C_g
No SOE	1.5	104
Spherical dome	1.5	257
SILO	1.2	248
XTP	1.3	425
RTP	0.85	677
FK	1.0	1,057
F-RXI	1.4	2,300
F-RXI*	1.4	1,750

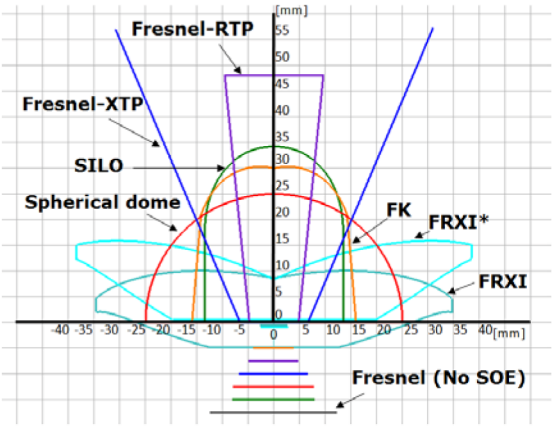

Fig. 8. Cross section of the SOE of the concentrators being compared. All these concentrators have the same POE entry aperture area (625 cm^2) and the same acceptance angle (α = ± 1°). The cross sections of their corresponding cells, which should be centered at the origin, are shown displaced downward to make them visible. *f*-numbers and geometrical concentrations are given in the left hand side.

#183585 - $15.00 USD Received 16 Jan 2013; revised 11 Mar 2013; accepted 12 Mar 2013; published 22 Apr 2013

A comparison of the concentration-acceptance angle product (*CAP*) for the selected concentrators is shown in Fig. 9. We can see that the FK and F-RXI concentrators are superior to all the conventional Fresnel-based concentrators described.

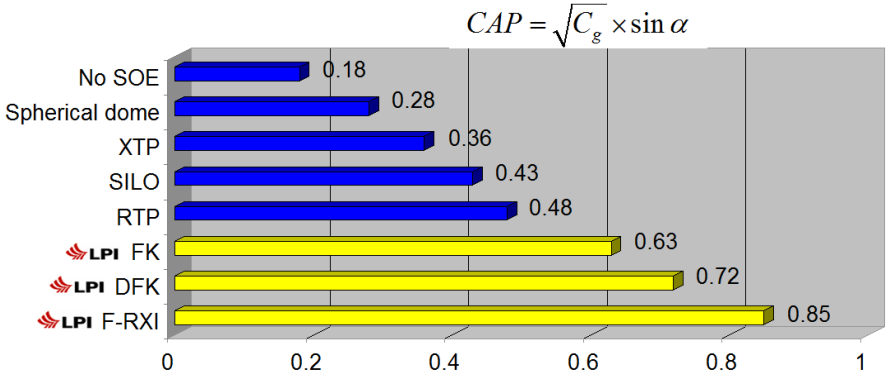

Fig. 9. Concentration acceptance angle product (*CAP*) for the concentrators under comparison.

5. Conclusions

The present challenge for CPV to finally enter the alternative energy generating market with volumetric success depends on its ability to demonstrate reliability and cost effectiveness, with the conventional fossil sources being the real benchmark in this case. Current CPV systems need to improve their performance (meaning energy, not power) and to reduce their costs at the same time. The FK and F-RXI concentrators are excellent candidates to achieve such improvements, due not only to their superior optical performance but to the practical aspects of high yield under mass-production conditions.

The FK *CAP* outperforms the conventional Fresnel-based CPV systems. This means that either its higher C_g or its higher tolerance angle α or both can be used to reduce cost. Moreover, its SOE design provides easy ways to protect the cell and relaxes most of the encapsulation issues found in conventional SOEs both things promoting a further cost reduction.

The F-RXI *CAP* outperforms the FK's but it is probably more expensive to manufacture, since it needs to be mirrored (like the secondaries of the Cassegrain-type systems). However, its ultra high *CAP* can be used to accommodate more expensive and more efficient cells, which will eventually be developed in the future.

The FK is already on the market and has proven (experimentally) module electrical (DC) efficiencies over 32.7%. Currently a dome-shaped FK prototype is being manufactured and tested. This DFK concentrator has a *CAP* (*CAP* = 0.72), higher than that of the FK and almost equal to that of the F-RXI*. Its SOE is as simple as the one in the conventional (flat Fresnel lens) FK, but its dome-shaped Fresnel lens is more complex.

Acknowledgments

The authors thank the European Commission (SMETHODS: FP7-ICT-2009-7 Grant Agreement No. 288526,: FP7-ENERGY.2011.1.1 Grant Agreement No. 283798), the Spanish Ministries (ENGINEERING METAMATERIALS: CSD2008-00066, DEFFIO: TEC2008-03773, ECOLUX: TSI-020100-2010-1131, SEM: TSI-020302-2010-65 SUPERRESOLUCION: TEC2011-24019, SIGMAMODULOS: IPT-2011-1441-920000, PMEL: IPT-2011-1212-920000), and UPM (Q090935C59) for the support given to the research activity of the UPM-Optical Engineering Group, making the present work possible.

#183585 - $15.00 USD Received 16 Jan 2013; revised 11 Mar 2013; accepted 12 Mar 2013; published 22 Apr 2013